11118 *Inorg. Chem.* **2010**, *49*, 11118–11126
DOI: 10.1021/ic101702b

Inorganic Chemistry
Article

Stabilization of 3:1 Site-Differentiated Cubane-Type Clusters in the $[Fe_4S_4]^{1+}$ Core Oxidation State by Tertiary Phosphine Ligation: Synthesis, Core Structural Diversity, and $S = 1/2$ Ground States

Liang Deng, Amit Majumdar, Wayne Lo, and R. H. Holm*

Department of Chemistry and Chemical Biology, Harvard University, Cambridge, Massachusetts 02138, United States

Received August 21, 2010

An extensive series of 3:1 site-differentiated cubane-type clusters $[Fe_4S_4(PPr^i_3)_3L]$ (L = Cl^-, Br^-, I^-, RO^-, RS^-, RSe^-) has been prepared in 40−80% yield by two methods: ligand substitution of $[Fe_4S_4(PPr^i_3)_4]^{1+}$ in tetrahydrofuran (THF)/acetonitrile by reaction with monoanions, and reductive cleavage of ligand substrates (RSSR, RSeSeR, I_2) by the all-ferrous clusters $[Fe_8S_8(PPr^i_3)_6]$/$[Fe_{16}S_{16}(PPr^i_3)_8]$ in THF. These neutral clusters are stable and do not undergo ligand redistribution reactions involving charged species in benzene and THF solutions. X-ray structural studies confirm the cubane stereochemistry but with substantial and variable distortions of the $[Fe_4S_4]^{1+}$ core from idealized cubic core geometry. Based on Fe−S bond lengths, seven clusters were found to have compressed tetragonal distortions (4 short and 8 long bonds), and the remaining seven display other types of distortions with different combinations of long, short, and intermediate bond lengths. These results further emphasize the facile deformabililty of this core oxidation state previously observed in $[Fe_4S_4(SR)_4]^{3-}$ clusters. The $Fe^{2.25+}$ mean oxidation state was demonstrated from ^{57}Fe isomer shifts, and the appearance of two quadrupole doublets arises from the spin-coupled $|9/2,4,1/2\rangle$ state. The $S = 1/2$ ground state was further supported by electron paramagnetic resonance spectra and magnetic susceptibility data.

Introduction

The fundamental chemistry and biomimetic advantages of cubane-type Fe_4S_4 clusters have been substantially expanded by the synthesis of 3:1 site-differentiated clusters in which one iron site is rendered unique by ligand design.[1] The original concept is illustrated by the structure of the cluster $[Fe_4S_4(LS_3)Cl]^{2-}$ in Figure 1.[2] The semirigid cavitand-like trithiolate ligand LS_3 binds the cluster at three sites, thereby differentiating a fourth site. Ligands at this site are often subject to facile substitution by a wide variety of other ligands to generate an extensive set of 3:1 site-differentiated clusters. Among other properties, this feature makes possible covalent coupling of two clusters or one cluster and another metal-containing entity such as a heme group, allows modulation of redox potentials and examination of the reactivity of coordinated ligands, and enables the $Fe_4S_4 \rightarrow Fe_3S_4$ cluster conversion by removal of the unique iron atom and thereafter formation of MFe_3S_4 clusters by binding of heterometals at the voided site. These and other applications of site-differentiated LS_3 clusters have been summarized.[1,3−5] Since the orginal report of $[Fe_4S_4(LS_3)Cl]^{2-}$ and related clusters, other 3:1 site-differentiated clusters based on different ligand platforms with three thiolate binding sites have been described[6−12] and one crystallographic structure proof has been provided.[6]

Clusters derived from the LS_3 ligand system have performed admirably in nearly all respects in the elucidation of site-differentiated Fe_4S_4 chemistry. The continued employment of this ligand does, however, raises several considerations. The ligand is the product of a multistep synthesis[2] which, although subsequently improved,[13] is somewhat lengthy. The lower core oxidation states $[Fe_4S_4]^{1+,0}$ are not readily achieved within the LS_3 framework. Reduction of the clusters $[Fe_4S_4(LS_3)L']^{2-}$

---

*To whom correspondence should be addressed. E-mail: holm@chemistry.harvard.edu.

[1] Rao, P. V.; Holm, R. H. *Chem. Rev.* **2004**, *104*, 527–559.

[2] Stack, T. D. P.; Holm, R. H. *J. Am. Chem. Soc.* **1988**, *110*, 2484–2494.

[3] Holm, R. H. Iron-Sulfur Clusters. In *Bio-coordination Chemistry*; Que, L., Jr., Tolman, W. A., Eds.; Elsevier: Oxford, 2004; pp 61−90.

[4] Holm, R. H. *Pure Appl. Chem.* **1998**, *70*, 931–938.

[5] Holm, R. H.; Ciurli, S.; Weigel, J. A. *Prog. Inorg. Chem.* **1990**, *38*, 1–74.

[6] Walsdorff, C.; Saak, W.; Pohl, S. *J. Chem. Soc., Dalton Trans.* **1997**, 1857–1861.

[7] Walsdorff, C.; Saak, W.; Haase, D.; Pohl, S. *J. Chem. Soc., Chem. Commun.* **1997**, 1931–1932.

[8] Evans, D. J.; Garcia, G.; Leigh, G. J.; Newton, M. S.; Santana, M. D. *J. Chem. Soc., Dalton Trans.* **1992**, 3229–3234.

[9] van Strijdonck, G. P. F.; van Haare, J. A. E. H.; van der Linden, J. G. M.; Steggerda, J. J.; Nolte, R. J. M. *Inorg. Chem.* **1994**, *33*, 999–1000.

[10] van Strijdonck, G. P. F.; van Haare, J. A. E. H.; Hönen, P. J. M.; van den Schoor, R. C. G. M.; Feiters, M. C.; van der Linden, J. G. M.; Steggerda, J. J.; Nolte, R. J. M. *J. Chem. Soc., Dalton Trans.* **1997**, 449–461.

[11] van Strijdonck, G. P. F.; ten Have, P. T. J. H.; Feiters, M. C.; van der Linden, J. G. M.; Steggerda, J. J.; Nolte, R. J. M. *Chem. Ber.* **1997**, *130*, 1151–1157.

[12] Whitener, M. A.; Peng, G.; Holm, R. H. *Inorg. Chem.* **1991**, *30*, 2411–2417.

[13] Stack, T. D. P.; Weigel, J. A.; Holm, R. H. *Inorg. Chem.* **1990**, *29*, 3745–3760.

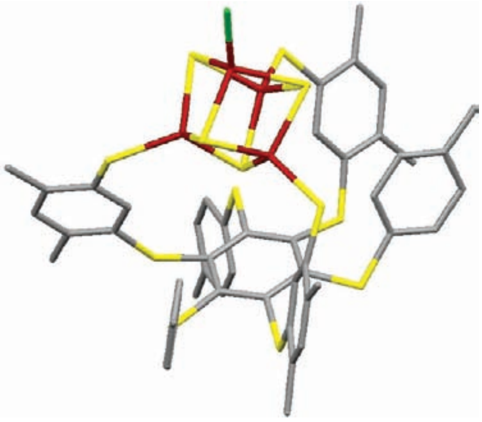

Figure 1. Structure of the 3:1 site-differentiated cluster $[Fe_4S_4(LS_3)Cl]^{2-}$ (LS_3 = 1,3,5-tris((4,6-dimethyl-3-mercaptophenyl)-thio)-2,4,6-tris(*p*-tolylthio)-benzene(3-)). The ligand is in the *aaabaa* conformation with one substituent below the plane of the central benzene ring.

to the $[Fe_4S_4]^{1+}$ level requires potentials < 1.0 V versus SCE, affording products highly susceptible to oxidation. While several clusters $[Fe_4S_4(LS_3)(SR)]^{3-}$ have been obtained in substance,[14] isolation of reduced clusters in pure crystalline form has proven difficult. Clusters in the all-ferrous $[Fe_4S_4]^0$ oxidation state are not accessible in this anionic ligand environment because of their oxidative instability. Solubility of cluster salts is restricted to solvents such as acetonitrile, dimethylformamide (DMF), and Me_2SO. Clusters formed from other site-differentiating ligands are unlikely to avoid these issues.

Previous research has shown that terminal phosphine or *N*-heterocyclic carbene ligation is effective in stabilization of the reduced states $[Fe_4S_4]^{1+,0}$.[15−17] In the course of this work, several clusters of the $[Fe_4S_4(PR_3)_3L]$ type with the $[Fe_4S_4]^{1+}$ oxidation state were isolated.[16] These are isoelectronic with $[Fe_4S_4(PBu^t_3)_3X]$ (X = halide) prepared by a different method[18] All of these species are 3:1 site-differentiated clusters prepared without benefit of a ligand designed for that purpose.[18] They offer the potential for investigation of the reactivity of reduced clusters—a matter explored fully only for electron transfer processes—including formation of higher nuclearity reduced clusters by coupling reactions and enhanced oxidation state stability by phosphine/carbene substitution. We report here the first detailed investigation of the synthesis and structures of 3:1 site-differentiated clusters of the $[Fe_4S_4(PR_3)_3L]$ type.

Experimental Section

Preparation of Compounds. All reactions and manipulations were performed under a pure dinitrogen atmosphere using either Schlenk techniques or an inert atmosphere box. Solvents were passed through an Innovative Technology solvent purification system prior to use. Solvent removal steps were performed in vacuo. All new compounds (13 single cubane, 2 double cubane clusters) were identified by ^1H NMR spectroscopy and crystal structure determinations; several compounds were further established by elemental analysis (Kolbe Microanalytical Laboratory, Mulheim, Germany). The compounds are soluble in non-polar or weakly polar solvents such as benzene, toluene, and tetrahydrofuran (THF) and are extremely air-sensitive and must be handled accordingly.

Chart 1. Designation of Clusters

$[Fe_4S_4(PPr^i_3)_4]^{1+}$	**1**[16]
$[Fe_8S_8(PPr^i_3)_6]$	**2**[15,16]
$[Fe_{16}S_{16}(PPr^i_3)_8]$	**3**[16]
$[Fe_4S_4(PPr^i_3)_3X]$	X = Cl^- **4**, Br^- **5**, I^- **6**
$[Fe_4S_4(PPr^i_3)_3(OR)]$	R = $SiPh_3$ **7**, $SiMe_2Bu^t$ **8**
$[Fe_4S_4(PPr^i_3)_3(SR)]$	R = Ph[16] **9**, C_6H_4-*p*-Me **10**, C_6H_4-*p*-OMe **11** C_6H_4-*p*-Cl **12**, $COCH_2Ph$ **13** $SiPr^i_3$ **14**, $SiPh_3$ **15**
$[Fe_4S_4(PPr^i_3)_3(SeR)]$	R = Ph **16**, C_6H_4-*p*-Cl **17**
$[Fe_8S_8(PPr^i_3)_4(OSiPh_3)_2]$	**18**
$[Fe_8S_8(PPr^i_3)_4(SR)_2]$	R = $Si(PPr^i_3)_3$ **19**, $SiPh_3$[16] **20**

$[Fe_8S_8(PPr^i_3)_6]$. The following procedure is more efficient than that reported earlier.[16] To a solution of $[FeCl_2(PPr^i_3)_2]$ (0.45 g, 1.0 mmol; prepared by the method for $[FeCl_2(PEt_3)_2]$[19]) in THF (10 mL) was added $(Me_3Si)_2S$ (0.27 g, 1.5 mmol). The reaction mixture was stirred for 2 d, solvent was removed, and the deep brown oily residue was dissolved in THF (5 mL). The solution was filtered. Vapor diffusion of *n*-hexane into the filtrate afforded the product as a brown crystalline solid (0.12 g, 57%) whose ^1H NMR spectrum is identical to that of an authentic sample.[16]

$[Fe_4S_4(PPr^i_3)_4](BF_4)$. To a solution of $[Fe_8S_8(PPr^i_3)_6]$ (0.166 g, 0.10 mmol) and PPr^i_3 (0.048 g, 0.30 mmol) in THF/acetonitrile (1:1 v/v, 5 mL) was added $[Cp_2Fe](BF_4)$ (0.055 g, 0.20 mmol). The reaction mixture was stirred overnight, and solvent was removed. The deep brown residue was washed with *n*-hexane (10 mL) and dissolved in THF (3 mL). The solution was filtered, and *n*-hexane (15 mL) was layered on the brown filtrate. The product was collected as a deep brown crystalline solid (0.15 g, 70%). ^1H NMR (CD_3CN): δ 2.31 (6), 5.08 (1). The cation spectrum is identical to that of the BPh_4^- salt.[16]

Site-Differentiated Clusters. 1. Ligand Substitution. $[Fe_4S_4(PPr^i_3)_3Cl]$. To a solution of $[Fe_4S_4(PPr^i_3)_4](BPh_4)$ (0.13 g, 0.099 mmol) in THF (5 mL) was added a solution of Ph_4PCl (0.038 g, 0.10 mmol) in acetonitrile (5 mL). The reaction mixture was stirred for 1 h, filtered, and solvent removed from the filtrate. The deep brown residue was extracted with a solution of Pr^i_3P (0.10 g, 0.62 mmol) in THF (3 mL), and the extract was filtered. Vapor diffusion of *n*-hexane into the filtrate afforded the product as a deep brown crystalline solid (0.044 g, 52%). ^1H NMR (C_6D_6): δ 1.90 (6), 2.88(1).

$[Fe_4S_4(PPr^i_3)Br]$. The preceding method on the same scale was used but with Ph_4PBr as the halide source. The product was obtained as a black-brown crystalline solid (0.050 g, 55%). Anal. Calcd. for $C_{27}H_{63}BrFe_4P_3S_4$: C, 35.55; H, 6.96; Fe, 24.49. Found: C, 35.53; H, 6.81; Fe, 24.42. ^1H NMR (C_6D_6): δ 1.91 (6), 2.86 (1).

$[Fe_4S_4(PPr^i_3)_3(OSiPh_3)]$. Method A. To a solution of $[Fe_4S_4(PPr^i_3)_4](BPh_4)$ (0.13 g, 0.099 mmol) in THF (5 mL) was added a solution of $NaOSiPh_3$ (0.030 g, 0.10 mmol; from Ph_3SiOH and NaH in THF) in acetonitrile (5 mL). The reaction mixture was stirred overnight, solvent was removed, and the deep brown residue was extracted with a solution of Pr^i_3P (0.10 g, 0.62 mmol) in benzene (5 mL). The extract was filtered, and the filtrate was reduced to 3 mL. The product separated as a brown crystalline solid (0.066 g,

---

[14] Daley, C. J. A.; Holm, R. H. *J. Inorg. Biochem.* **2003**, *97*, 287–298.

[15] Goh, C.; Segal, B. M.; Huang, J.; Long, J. R.; Holm, R. H. *J. Am. Chem. Soc.* **1996**, *118*, 11844–11853.

[16] Zhou, H.-C.; Holm, R. H. *Inorg. Chem.* **2003**, *42*, 11–21.

[17] Deng, L.; Holm, R. H. *J. Am. Chem. Soc.* **2008**, *130*, 9878–9886.

[18] Tyson, M. A.; Demadis, K. D.; Coucouvanis, D. *Inorg. Chem.* **1995**, *34*, 4519–4520.

[19] Booth, G.; Chatt, J. *J. Chem. Soc.* **1962**, 2099–2106.

Table 1. Crystallographic Data for $[Fe_4S_4]^{1+}$ complexes (**4**−**11**) at 100 K^a

	4	**5**	**6**	**7**	**8**	**9**	**10**	**11**
formula	$C_{27}H_{63}ClFe_4P_3S_4$	$C_{27}H_{63}BrFe_4P_3S_4$	$C_{27}H_{63}Fe_4IP_3S_4$	$C_{45}H_{78}Fe_4OP_3S_4Si$	$C_{33}H_{78}Fe_4OP_3S_4Si$	$C_{33}H_{68}Fe_4P_3S_5$	$C_{34}H_{70}Fe_4P_3S_5$	$C_{34}H_{70}Fe_4OP_3S_5$
formula weight	867.77	912.26	959.26	1107.76	963.62	941.53	955.55	971.56
crystal system	monoclinic	monoclinic	monoclinic	trigonal	triclinic	monoclinic	monoclinic	monoclinic
space group	$P2_1/c$	$P2_1/c$	$P2_1/c$	$P\bar{3}c1$	$P\bar{1}$	$P2_1/c$	$P2_1/c$	$P2_1/n$
Z	4	4	4	4	2	4	4	4
a, Å	10.7153(11)	15.5180(5)	15.757(2)	16.1863(7)	12.0082(4)	16.426 (3)	16.809 (5)	19.3706 (7)
b, Å	22.869(2)	13.3790(4)	13.5181(17)	16.1863(7)	12.0826(4)	13.714 (3)	13.094 (4)	11.2553 (4)
c, Å	16.6553(17)	18.8744(6)	18.911(2)	25.7751(18)	19.6232(7)	19.960 (4)	19.838 (5)	21.7355 (8)
α, deg	90.00	90.00	90.00	90.00	88.265(2)	90.00	90.00	90.00
β, deg	102.720(2)	97.874(2)	97.816(2)	90.00	76.221(2)	100.182(5)	92.556 (5)	110.238 (1)
γ, deg	90.00	90.00	90.00	120.00	62.209(2)	90.00	90.00	90.00
V, Å^3	3981.1(7)	3881.7(2)	3990.9(9)	5848.3(5)	2435.41(14)	4425.6 (14)	4362 (2)	4446.3 (3)
d_{calcd}, g/cm^3	1.403	1.561	1.597	1.258	1.314	1.413	1.450	1.451
μ, mm^{-1}	1.841	2.851	2.546	1.247	1.485	1.652	1.677	1.648
2θ range, deg	4.34−52.50	4.40−51.92	4.34−51.60	5.02−56.5	4.56−56.74	4.62 −50.86	4.39−42.67	4.36−51.87
$R_1{}^b$ ($wR_2{}^c$)	0.0488 (0.1174)	0.0312 (0.0760)	0.0657 (0.1763)	0.0239 (0.0755)	0.0296 (0.0788)	0.0473 (0.0961)	0.1225 (0.3102)	0.0287 (0.0716)
GOF (F^2)	1.056	1.063	1.171	1.206	1.035	0.986	1.139	1.071

^{a} Mo Kα radiation ($\lambda = 0.71073$ Å). ^{b} $R_1 = \sum||F_o| - |F_c||/\sum|F_o|$. ^{c} $wR_2 = \{\sum w(F_o{}^2 - F_c{}^2)^2/\sum w(F_o{}^2)^2\}^{1/2}$.

Table 2. Crystallographic Data for $[Fe_4S_4]^{1+}$ complexes (**12**− **19**) at 100 K^a

	12	**13**	**14**	**15**	**16**	**17**	**18**	**19**
formula	$C_{33}H_{67}ClFe_4P_3S_5$	$C_{35}H_{70}Fe_4OP_3S_5$	$C_{36}H_{84}Fe_4P_3S_5Si$	$C_{45}H_{78}Fe_4P_3S_5Si$	$C_{33}H_{68}Fe_4P_3S_4Se$	$C_{33}H_{67}Fe_4P_3S_4SeCl$	$C_{72}H_{114}Fe_8O_2P_4S_8Si$	$C_{54}H_{126}Fe_8P_4S_{10}Si_2$
formula weight	975.98	983.57	1021.73	1123.83	988.42	1022.85	1895.05	1723.11
crystal system	monoclinic	triclinic	triclinic	monoclinic	triclinic	monoclinic	monoclinic	triclinic
space group	$P2_1/c$	$P\bar{1}$	$P\bar{1}$	$P2_1/c$	$P\bar{1}$	$P2_1/n$	$P2_1/c$	$P\bar{1}$
Z	4	2	2	4	2	4	2	2
a, Å	14.096 (2)	11.220 (2)	10.890(3)	19.805(4)	11.1659(13)	24.168(4)	11.2573(14)	13.383(12)
b, Å	19.807 (3)	13.240 (2)	13.723(4)	10.671(3)	11.3089(13)	17.033(3)	28.095(4)	13.635(12)
c, Å	17.396 (3)	17.784 (3)	18.892(6)	27.592(6)	17.666(2)	24.185(4)	14.5028(18)	14.548(13)
α, deg	90.00	98.113 (3)	99.753(5)	90.00	85.122(2)	90.00	90.00	62.452(12)
β, deg	112.598 (2)	102.382 (3)	103.788(4)	109.978(4)	88.949(2)	113.507(3)	106.781(2)	65.944(13)
γ, deg	90.00	114.675 (2)	106.327(4)	90.00	79.238(2)	90.00	90.00	62.296(12)
V, Å^3	4484.1 (12)	2264.2 (7)	2545.3(14)	5480(2)	2183.6(4)	9130(3)	4391.5(9)	2020(3)
d_{calcd}, g/cm^3	1.446	1.443	1.333	1.362	1.503	1.489	1.433	1.417
μ, mm^{-1}	1.690	1.619	1.464	1.367	2.459	2.412	1.612	1.792
2θ range, deg	4.82−51.48	4.516−51.46	4.58−55.68	4.36−48.42	4.38−51.73	4.38−50.46	4.98−46.48	5.36−56.46
$R_1{}^b$ ($wR_2{}^c$)	0.0348 (0.0786)	0.0395 (0.1019)	0.0729 (0.1753)	0.0440 (0.1001)	0.0653 (0.1840)	0.0696 (0.1752)	0.0381 (0.0606)	0.0363 (0.0880)
GOF (F^2)	1.081	1.054	1.020	1.010	1.039	1.026	0.758	1.029

^{a} Mo Kα radiation ($\lambda = 0.71073$ Å). ^{b} $R_1 = \sum||F_o| - |F_c||/\sum|F_o|$. ^{c} $wR_2 = \{\sum w(F_o{}^2 - F_c{}^2)^2/\sum w(F_o{}^2)^2\}^{1/2}$.

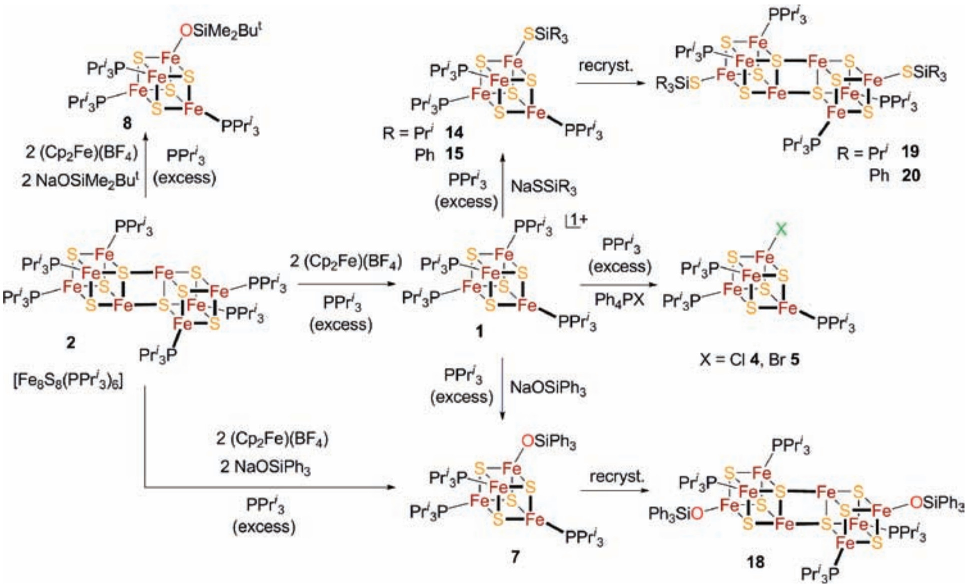

Figure 2. Schematic depiction of the synthesis of clusters by phosphine ligand substitution of **1**.

60%). ^{1}H NMR ($\mathrm{C_6D_6}$): δ 1.88 (18), 3.07 (3), 7.27 (t, 1), 7.84 (d, 2), 8.75 (br, 2).

Method B. To a solution of $[\mathrm{Fe_8S_8(PPr}^i_3)_6]$ (0.17 g, 0.010 mmol) and PPr^i_3 (0.10 g, 0.62 mmol) in THF/acetonitrile (1:1 v/v, 5 mL) was added $[\mathrm{Cp_2Fe}](\mathrm{BF_4})$ (0.055 g, 0.20 mmol) and $\mathrm{NaOSiPh_3}$ (0.060 g, 0.20 mmol). The reaction mixture was stirred overnight and solvent was removed. Vapor diffusion of *n*-hexane into the reddish-brown filtrate yielded the product as brown crystals (0.044 g, 20%). The ^{1}H NMR spectrum is identical to that of the product of Method A.

$[\mathrm{Fe_4S_4(PPr}^i_3)_3(\mathrm{OSiMe_2Bu}^t)]$. Method B of the preceding preparation was employed on the same scale with use of $\mathrm{NaOSiMe_2Bu}^t$. After being stirred overnight, the reaction mixture was reduced to a deep brown residue, which was extracted with a solution of $\mathrm{Pr}^i_3\mathrm{P}$ (0.10 g, 0.62 mmol) in benzene (5 mL). Removal of solvent from the extract filtrate afforded the product as a brown crystalline solid (0.097 g, 50%). ^{1}H NMR ($\mathrm{C_6D_6}$): δ 1.14 (2), 1.97 (18), 2.61 (3), 3.58 (3).

$[\mathrm{Fe_8S_8(PPr}^i_3)_4(\mathrm{OSiPh_3})_2]$. Vapor diffusion of *n*-hexane into a solution of $[\mathrm{Fe_4S_4(PPr}^i_3)_3(\mathrm{OSiPh_3})]$ (0.050 g, 0.045 mmol) in benzene (4 mL) over 2−3 d caused separation of the product as a brown crystalline solid (0.038 g, 45%). H NMR ($\mathrm{C_6D_6}$): δ 1.90 (2), 3.06 (br, 12), 6.78 (2), 7.3 (~1), 7.62 (2).

$[\mathrm{Fe_4S_4(PPr}^i_3)_3(\mathrm{SSiPr}^i_3)]$. To a solution of $[\mathrm{Fe_4S_4(PPr}^i_3)_4](\mathrm{BPh_4})$ (0.13 g, 0.099 mmol) in THF (5 mL) was added a solution of $\mathrm{NaSSiPr}^i_3$ (0.021 g, 0.099 mmol; from $\mathrm{Pr}^i_3\mathrm{SiSH}$ and NaH in THF) in acetonitrile (5 mL). The reaction mixture was stirred overnight, and solvent was removed. The deep brown residue was extracted with a solution of $\mathrm{Pr}^i_3\mathrm{P}$ (0.10 g, 0.62 mmol) in benzene (7 mL), and the solution was filtered. Reduction of the solution to about 1 mL caused separation of the product as a brown crystalline solid (0.072 g, 71%). ^{1}H NMR ($\mathrm{C_6D_6}$): δ 1.98 (18), 2.71 (6), 3.40 (3) 4.61 (1). Anal. Calcd. for $\mathrm{C_{36}H_{84}Fe_4P_3S_5Si}$: C, 42.32; H, 8.29; Fe, 21.86; S, 15.69. Found: C, 41.24; H, 8.10: Fe, 21.30; S, 15.20.

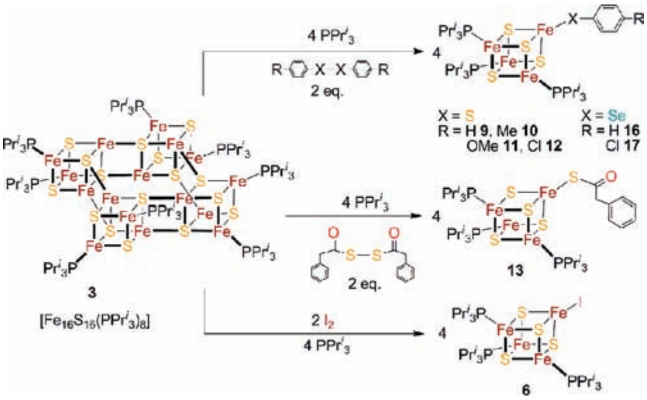

Figure 3. Schematic depiction of the synthesis of clusters by reductive cleavage of ligand precursors.

$[\mathrm{Fe_8S_8(PPr}^i_3)_4(\mathrm{SSiPr}^i_3)_2]$. Vapor diffusion of *n*-hexane into a solution of $[\mathrm{Fe_4S_4(PPr}^i_3)_3(\mathrm{SSiPr}^i_3)]$ (0.050 g, 0.049 mmol) in benzene (2 mL) afforded the product as brown crystals (0.034 g, 80%). ^{1}H NMR ($\mathrm{C_6D_6}$): δ 0.64 (6) 1.90 (1), 1.95 (2), 2.98 (12).

2. Reductive Cleavage. **$[\mathrm{Fe_4S_4(PPr}^i_3)_3(\mathrm{SPh})]$.** A solution of diphenyldisulfide (4.5 mg, 0.020 mmol) in THF (2 mL) was added to a solution of $[\mathrm{Fe_{16}S_{16}(PPr}^i_3)_8]$[16] (27 mg, 0.010 mmol) and PPr^i_3 (10 mg, 0.060 mmol) in THF (8 mL). The reaction mixture was stirred for 12 h to give a reddish-brown solution. Volatiles were removed, and the residue was extracted with benzene (1 mL) containing PPr^i_3 (20 mg, 0.12 mmol). Vapor diffusion of hexane over 1 d caused separation of the product as black-brown crystals (17 mg, 45%). ^{1}H NMR ($\mathrm{C_6D_6}$): δ −2.70 (1), −1.55 (br, 2), 1.94 (54), 3.10 (9), 13.04 (2). This spectrum is in agreement with an earlier report of this compound prepared by a self-assembly method.[16]

The following seven compounds were prepared on the same scale by the same method but with use of the different disulfides, and were isolated as black-brown crystals in the indicated yields.

$[\mathrm{Fe_4S_4(PPr}^i_3)_3(\mathrm{SC_6H_4}$-*p*-$\mathrm{Me})]$. Bis(*p*-tolyl)disulfide (5.0 mg, 0.020 mmol); 16 mg (42%). ^{1}H NMR ($\mathrm{C_6D_6}$): δ −1.85 (2), 1.94 (54), 3.09 (9), 12.01 (3), 12.94 (2).

$[\mathrm{Fe_4S_4(PPr}^i_3)_3(\mathrm{SC_6H_4}$-*p*-$\mathrm{Cl})]$. Bis(*p*-chlorophenyl)disulfide (5.8 mg, 0.020 mmol); 20 mg (50%). ^{1}H NMR ($\mathrm{C_6D_6}$): δ −1.79 (2), 1.92 (54), 3.00 (9), 12.92 (2). Anal. Calcd. for $\mathrm{C_{33}H_{67}ClFe_4P_3S_5}$: C, 40.61; H, 6.92; Fe, 22.89; S, 16.43. Found: C, 40.75; H, 6.82; Fe, 22.90; S, 16.22.

$[\mathrm{Fe_4S_4(PPr}^i_3)_3(\mathrm{SC_6H_4}$-*p*-$\mathrm{OMe})]$. Bis(*p*-methoxyphenyl)disulfide (5.6 mg, 0.020 mmol); 15 mg, (39%). ^{1}H NMR ($\mathrm{C_6D_6}$): δ −1.62 (2), 1.94 (54), 3.13 (9), 4.23 (3), 12.31 (2).

$[\mathrm{Fe_4S_4(PPr}^i_3)_3(\mathrm{SePh})]$. Diphenyldiselenide (6.2 mg, 0.020 mmol); 30 mg (75%). ^{1}H NMR ($\mathrm{C_6D_6}$): δ −2.70 (1), −1.52 (2), 1.94 (54), 3.07 (9), 11.86 (2).

$[\mathrm{Fe_4S_4(PPr}^i_3)_3(\mathrm{SeC_6H_4}$-*p*-$\mathrm{Cl})]$. Bis(*p*-chlorophenyl)diselenide (7.6 mg, 0.020 mmol); 27 mg (66%). ^{1}H NMR ($\mathrm{C_6D_6}$): δ −1.78 (1), 1.93 (54), 3.00 (9), 11.63 (2). *Anal.* Calcd. for $\mathrm{C_{33}H_{67}ClFe_4P_3S_4Se}$: C, 38.75; H, 6.60; Fe, 21.84; S, 12.54. Found: C, 36,.12; H, 6.17; Fe, 21.32; S, 12.29.

$[\mathrm{Fe_4S_4(PPr}^i_3)_3\mathrm{I}]$. Iodine (2.5 mg, 0.020 mmol); 13 mg (34%). ^{1}H NMR ($\mathrm{C_6D_6}$): δ 1.94 (54), 2.91 (9). Anal. Calcd. for $\mathrm{C_{45}H_{78}Fe_4IP_3S_4}$: C, 33.81; H, 6.62; Fe, 23.29; S, 13.37. Found: C, 33.60; H, 6.55; Fe, 23.10; 13.20.

$[\mathrm{Fe_4S_4(PPr}^i_3)_3(\mathrm{SCOCH_2Ph})]$. Bis(phenylacetyl)disulfide (6.0 mg, 0.020 mmol); 16 mg (41%).

In the sections following, clusters are numerically designated according to Chart 1.

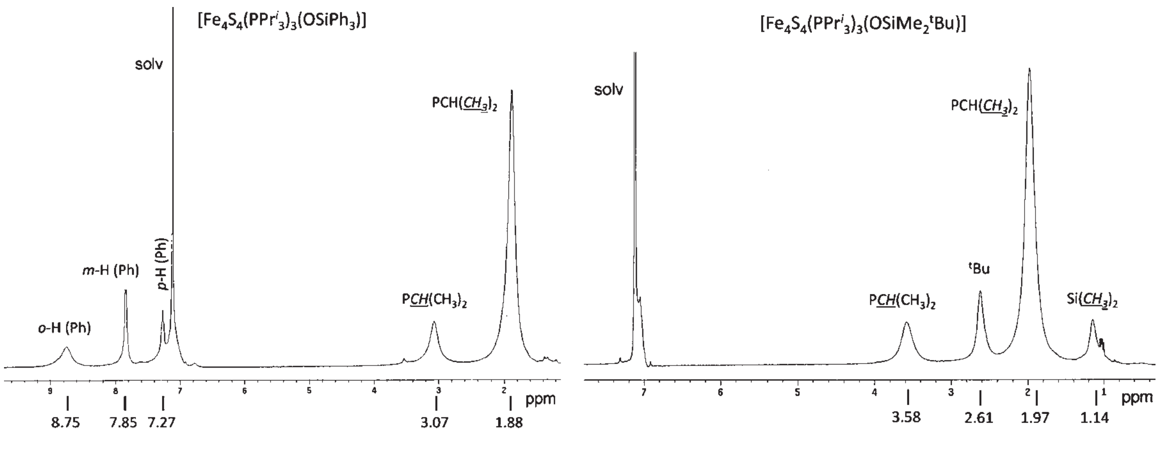

Figure 4. H NMR spectra of representative clusters **7** (left) and **8** in $\mathrm{C_6D_6}$. Signal assignments are indicated.

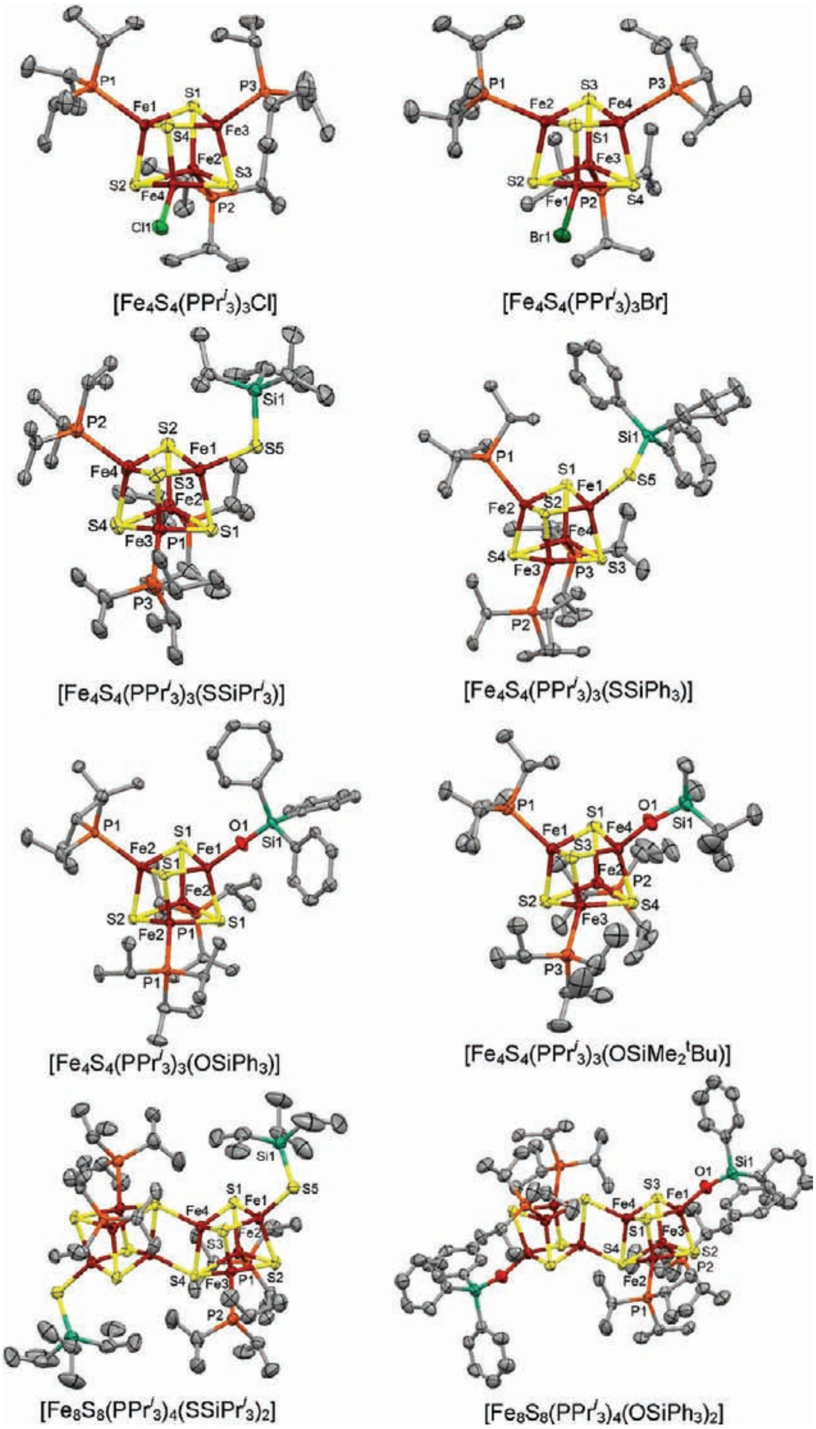

[Fe$_4$S$_4$(PPr$^i_3$)$_3$Cl] [Fe$_4$S$_4$(PPr$^i_3$)$_3$Br]

[Fe$_4$S$_4$(PPr$^i_3$)$_3$(SSiPr$^i_3$)] [Fe$_4$S$_4$(PPr$^i_3$)$_3$(SSiPh$_3$)]

[Fe$_4$S$_4$(PPr$^i_3$)$_3$(OSiPh$_3$)] [Fe$_4$S$_4$(PPr$^i_3$)$_3$(OSiMe$_2{}^t$Bu)]

[Fe$_8$S$_8$(PPr$^i_3$)$_4$(SSiPr$^i_3$)$_2$] [Fe$_8$S$_8$(PPr$^i_3$)$_4$(OSiPh$_3$)$_2$]

Figure 5. Structures of single cubanes (**4**, **5**, **7**, **8**, **14**, **15**) prepared by phosphine ligand substitution and double cubanes (**18**, **19**) obtained by phosphine dissociation from single cubanes. Both types are shown with 50% probability ellipsoids and partial atom numbering schemes. Double cubanes have crystallographically imposed centrosymmetry.

X-ray Structure Determinations. The structures of the 16 compounds in Tables 1 and 2 were determined. Diffraction-quality crystals were obtained by hexane diffusion into THF (**4**, **5**) or benzene (**6**−**19**) solutions. Crystal mounting and data collections were performed as described[20] on a Siemens (Bruker) SMART CCD diffractometer using Mo Kα radiation. Data reductions were performed with SAINT, which corrects for Lorentz polarization and decay. Space groups were assigned by analysis of symmetry, and systematic absences were determined by XPREP and were further checked by PLATON. Structures were solved by direct methods and refined against all data in the 2θ ranges by full-matrix least-squares on F^2 using SHELXS-97 and SHELXL-97. Hydrogen atoms at idealized positions were included in final refinements. Refinement details and explanations (wherever necessary) are included in the individual CIF files. Crystallographic data and final agreement factors are given in Tables 1 and 2.[21]

---

[20] Groysman, S.; Holm, R. H. *Inorg. Chem.* **2007**, *46*, 4090–4102.

[21] See paragraph at the end of this article for Supporting Information available.

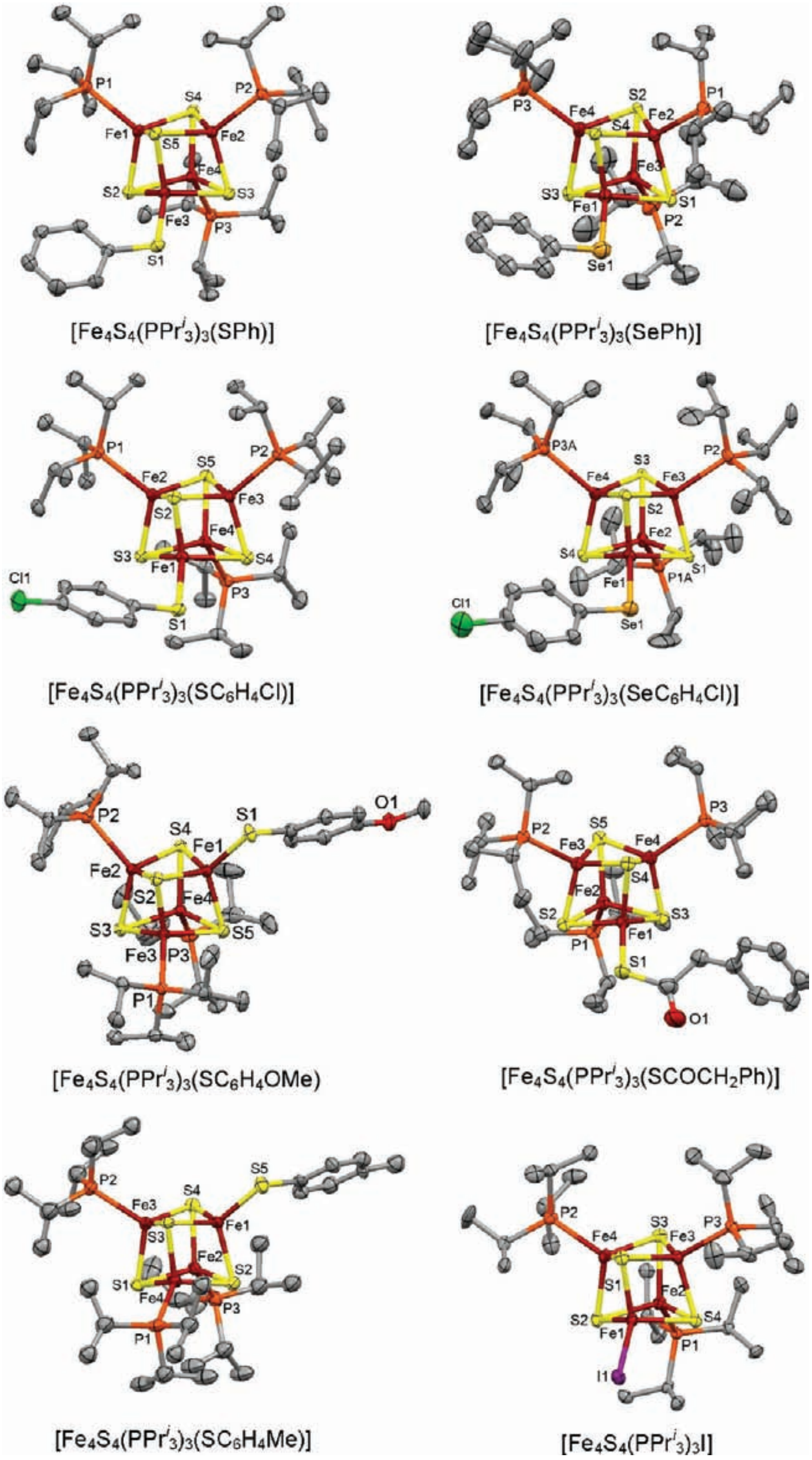

$[Fe_4S_4(PPr^i_3)_3(SPh)]$ $[Fe_4S_4(PPr^i_3)_3(SePh)]$

$[Fe_4S_4(PPr^i_3)_3(SC_6H_4Cl)]$ $[Fe_4S_4(PPr^i_3)_3(SeC_6H_4Cl)]$

$[Fe_4S_4(PPr^i_3)_3(SC_6H_4OMe)$ $[Fe_4S_4(PPr^i_3)_3(SCOCH_2Ph)]$

$[Fe_4S_4(PPr^i_3)_3(SC_6H_4Me)]$ $[Fe_4S_4(PPr^i_3)_3I]$

Figure 6. Structures of single cubanes (**6**, **9**−**13**, **16**, **17**) prepared by reductive cleavage showing 50% probability ellipsoids and partial atom labeling schemes.

Other Physical Measurements. ^{1}H NMR spectra were obtained with a Varian M400 spectrometer. Electron paramagnetic resonance (EPR) spectra in THF solutions were recorded on a Bruker ELEXSYS-II spectrometer operating at X-band and 4.5 K. ^{57}Fe Mössbauer spectra were measured with a constant acceleration spectrometer. Data were analyzed with WMOSS software (WEB Research, Edina, MN); isomer shifts are referenced to iron metal at room temperature. Magnetic susceptibility data were collected with a Quantum Design SQUID magnetometer at 1 T and 2−300 K (MIT Center for Materials Science and Engineering).

Results and Discussion

Synthesis of Clusters. The 3:1 site-differentiated clusters of general type $[Fe_4S_4(PR_3)_3L]$, in which R = Pr^i and L is a variant anionic ligand, are accessible by two procedures, phosphine ligand substitution and reductive cleavage

Table 3. Summary of Structural Parameters (Å) of the Clusters [$Fe_4S_4(PPr^i_3)_3L$] with the 4 Short +8 Long Fe−S Bond Length Pattern

L	SPh	SC_6H_4Cl	SC_6H_4OMe	$SCOCH_2Ph$	SePh	I	Br
core structures[a]	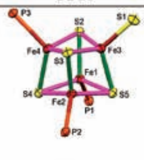	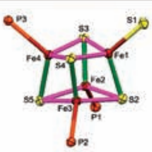	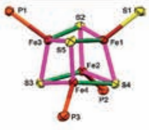	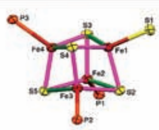	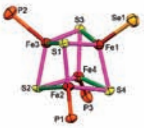	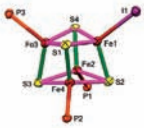	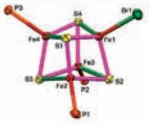
Fe − S	4s 2.228 (12)[b]	4s 2.216 (8)	4s 2.225 (6)	4s 2.224 (9)	4s 2.258 (13)	4s 2.223 (12)	4s 2.214 (15)
	8l 2.296 (15)	8l 2.294 (17)	8l 2.285 (19)	8l 2.292 (11)	8l 2.329 (13)	8l 2.286 (14)	8l 2.286 (14)
Fe − Fe	2.67 (2)	2.66(3)	2.66 (2)	2.67 (3)	2.68 (3)	2.68 (2)	2.67 (3)
Fe − L	2.270 (1)	2.268(1)	2.251(1)	2.279 (1)	2.373 (1)	2.566 (1)	2.357 (1)

[a] Bond color codes: green, short (s); magenta, long (l). [b] Standard deviation from mean.

Table 4. Summary of Structural Parameters (Å) of the Clusters [$Fe_4S_4(PPr^i_3)_3L$] with Other Core Distortions

L	Cl	$OSiMe_2{}^tBu$	$OSiPh_3$	SC_6H_4Me	$SSiPh_3$	$SSiPr^i_3$	SeC_6H_4Cl[d]
core structures[a]	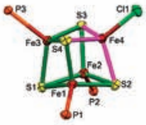	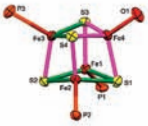	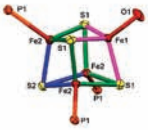	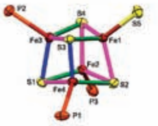	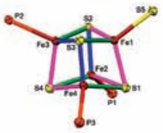	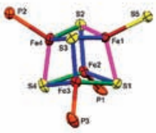	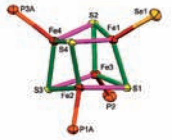
Fe − S			6s 2.276[c]	4s 2.211 (6)	4s 2.233 (16)	3s 2.235 (5)	
	9s 2.275 (9)[b]	6s 2.267 (4)					8s 2.288 (8)
			3i 2.285[c]	2i 2.249 (7)	3i 2.290 (2)	6i 2.284 (8)	
	3l 2.306 (2)	6l 2.303 (15)					4l 2.321 (13)
			3l 2.309[c]	6l 2.270 (10)	5l 2.320 (14)	3l 2.323 (12)	
Fe − Fe	2.699 (7)	2.71 (2)	2.71 (1)	2.66 (1)	2.70 (4)	2.70 (3)	2.69 (2)
Fe − L	2.234 (1)	1.830 (1)	1.837 (3)	2.233 (6)	2.287 (1)	2.285 (2)	2.369 (2)

[a] Bond color codes: green, short (s); blue, intermediate (i), magenta, long (l). [b] Standard deviation from mean. [c] Equal by symmetry. [d] A second independent unit in the asymmetric unit displays a 11s (2.298 (6)) + 1l (2.322(2)) Å Fe−S bond distance pattern.

of ligand precursors. Both originate with known all-ferrous precursors, the edge-bridged double cubane **2** or the tetracubane **3**. As shown in Figure 2, cluster **2** is oxidized with 2 equiv of $[Cp_2Fe]^+$ in acetonitrile/THF in the presence of added phosphine to the cationic cubane cluster **1**, isolable as the BF_4^- or BPh_4^- salt. Treatment of **1** with 1 equiv of ligand in reaction 1 yields halide clusters **4** and **5** and silylthiolate clusters **14** and **15**. Alternatively, oxidation of **2** in the presence of ligand in acetonitrile/THF without prior isolation of **1** affords silyloxide clusters **7** and **8** directly. In the reductive cleavage method of Figure 3, 2 equiv of substrate L_2 and 1 equiv of tetracubane **3** generate ligand monoanions which are captured by cubane fragments of **3** in reaction 2 (L = I, RS, RSe) to yield clusters **6**, **9**−**13**, **16**, and **17**.

$$[Fe_4S_4(PPr^i_3)_4]^{1+} + L^- \rightarrow [Fe_4S_4(PR_3)_3L] + PPr^i_3 \quad (1)$$

$$[Fe_{16}S_{16}(PPr^i_3)_8] + 2L_2 + 4PPr^i_3 \rightarrow 4[Fe_4S_4(PR_3)_3L] \quad (2)$$

Certain useful observations follow from these reactions. In ligand substitution with halides, it is desirable to utilize [**1**](BPh_4) and the Ph_4P^+ salt of the ligand anion owing to the favorably low solubility of (Ph_4P)(BPh_4) in the reaction medium. Workup procedures are performed in the presence of added phosphine to stabilize the desired single cubane products. These clusters have a propensity to liberate coordinated phosphine in reaction 3, leading to ready isolation of the less soluble edge-bridged double cubane. This behavior was demonstrated by isolation of

$$2[Fe_4S_4(PPr^i_3)_3L] \rightleftarrows [Fe_8S_8(PPr^i_3)_4L_2] + 2PPr^i_3 \quad (3)$$

double cubanes **18** (45%) and **19** (80%) from benzene/hexane solutions of **7** and **14**, respectively. Previously, cluster **20** had been isolated similarly from THF/ether.[16] The cluster reactant in reductive cleavage of L_2 may be in part **2** inasmuch as this cluster and **3** are in equilibrium in the presence of added phosphine used in the procedure. Clusters **2** and **3** are easily distinguished by ^1H NMR.[16]

Reactions 1 and 2 afford oxidatively sensitive single cubanes [$Fe_4S_4(PPr^i_3)_3L$] in 40−80% yields as crystalline solids soluble in benzene and THF to form red-brown solutions. Double cubanes are slightly soluble in benzene and quite soluble in THF and dichloromethane to give deep brown solutions. A small number of mixed-ligand anionic clusters $[Fe_4S_4L_{4-n}L'_n]^{2-}$ have been isolated as salts soluble in polar solvents such as acetonitrile or DMF; others have been generated in solution by ligand substitution. Without recourse to a site-differentiating ligand such as LS_3[1] (Figure 1), such species normally equilibrate by ligand exchange to mixtures of clusters, a behavior demonstrated early in the development of iron−sulfur clusters.[22] Inasmuch as similar reactions of [$Fe_4S_4(PPr^i_3)_3L$] would necessarily implicate charged

---

[22] Que, L., Jr.; Bobrik, M. A.; Ibers, J. A.; Holm, R. H. *J. Am. Chem. Soc.* **1974**, *96*, 4168–4178.

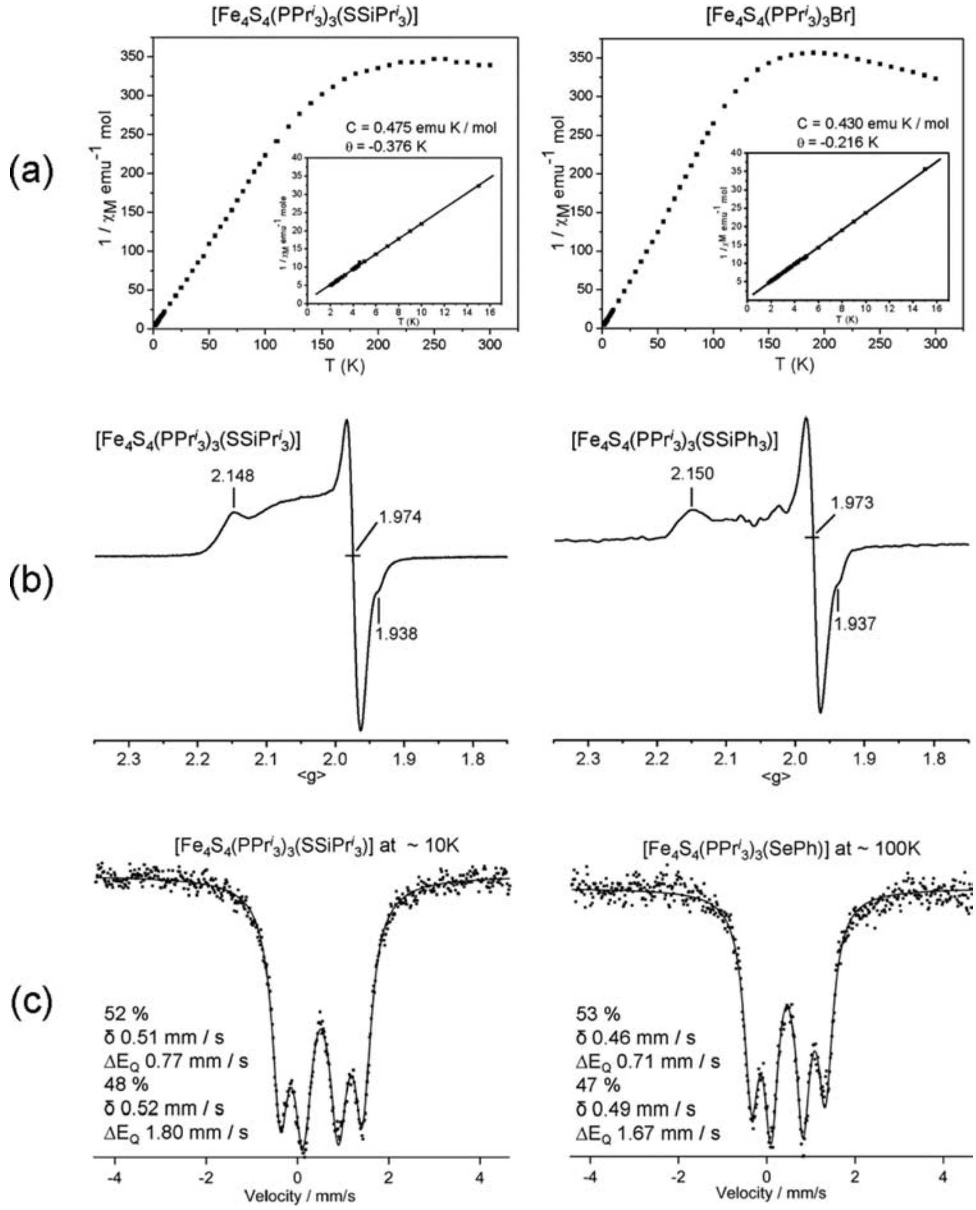

Figure 7. (a) Temperature dependence of the reciprocal molar susceptibility at $H = 1$ T; inset: Curie plot at 2−15 K with Curie and Weiss constants indicated. (b) X-band EPR spectra at 4.5 K in THF; apparent *g*-values are indicated ($g_{av} = 2.03$). (c) Zero-field Mössbauer spectra with isomer shifts (δ) and quadrupole splitting (ΔE_Q) indicated.

clusters, they are suppressed in low-polarity media, accounting for the stability of the neutral clusters. As examples, the paramagnetically shifted ^{1}H NMR spectra of clusters **7** and **8** in Figure 4 serve to identify them and demonstrate their stability in benzene.

Structures of Clusters. The cubane formulation of clusters $[Fe_4S_4(PPr^i_3)_3L]$ has been verified by the structures of clusters prepared by both methods and provided in Figures 5 and 6. Mean values of Fe−L bond lengths and Fe−S and Fe−Fe distances of the $[Fe_4S_4]^{1+}$ cores of these structures are collected in Table 3. Full sets of structural data are available elsewhere.[21] Individual bond distances and angles are unexceptional. The most significant structural aspect is the range of core distortions from the highest idealized core geometry, taken as T_d inasmuch as no weak field mixed-valence Fe_4S_4 cluster ever manifests localized Fe^{3+} or Fe^{2+} sites. Such species are always electronically delocalized. As shown in Tables 3 and 4, eight core distortion patterns are recognizable from Fe−S distances, which are designated as short (s), long (l), and intermediate (i) with color coding. These distances are sorted *within* in each structure rather than over the entire set with statistically defined limits, resulting in a qualitative description of distortions. The most prevalent of these is the 4s + 8l pattern observed for seven clusters (Table 3). The differences in mean values of 0.060−0.078 Å emphasize the extent of distortion, which takes the form of compressed tetragonal Fe_4S_4 core geometry that ideally conforms to an improper S_4 axis passing through the midpoints of the opposite Fe_2S_2 -core faces. Other distortion patterns, although less pronounced, are 9s + 3l and 6s + 6l. The remaining cases can be described in terms of s + i + l combinations (Table 4). Despite the nature of the ligand set, there are no cases of a strict trigonal distortion, although cluster **7** (6s + 3i + 3l) approaches that situation. The detailed structures of $[Fe_4S_4]^{3+,2+,1+}$ core structures in proteins and synthetic compounds and interpretations of distortions continues as a matter of current significance.[23,23] The purpose of the scheme presented here is to emphasize once again the deformability, or "plasticity", of the $[Fe_4S_4]^{1+}$ core. This property is dramatized by the occurrence of two very differently distorted cores, 8s + 4l and 1s + 11l, in the asymmetric unit of cluster **17**. Core deformability has also been revealed by structural investigations of $[Fe_4S_4(SR)_4]^{3-}$ clusters in which the terminal ligands are identical.[1,24−26] Over a dozen different distortions from cubic core symmetry have now been observed, including both elongated and compressed tetragonal structures and others, including some of those found here, for which there is no simple geometric description. Distortions are evidently produced by non-bonded interactions in the solid state and appear to reflect a soft potential surface with competing energy minima. By way of comparison, $[Fe_4S_4]^{2+}$ clusters also exhibit distortions from T_d idealized core geometry, the most frequently encountered of which is compressed tetragonal (4s + 8l).[1] It has been suggested that this structure is trapped by lattice effects in both proteins and crystalline analogue complexes and may revert to T_d symmetry in solution.[23] It remains of much interest to see what distortion(s) would be adopted by $[Fe_4S_4]^{1+}$ clusters in proteins. Unfortunately, no X-ray structures of reduced proteins are currently available.

Ground State Properties. Adequate characterization of $[Fe_4S_4]^{1+}$ clusters requires specification of ground state spin inasmuch as values of $S = 1/2$ to $7/2$ have been observed for synthetic and protein-bound species. Among the former, examples of pure $S = 1/2$ and $3/2$ as well as spin-admixed $S = 1/2 + 3/2$ states have been reported.[24−28] Data for representative clusters **5** and **14** are summarized in Figure 7. Magnetic susceptibilities adhere to the Curie−Weiss law $\chi^M = C/(T - \theta)$ at 2−15 K with Curie constants $C = 0.475$ and 0.430 emu K/mol, close to the theoretical value of $C = 0.375$ emu K/mol for $S = 1/2$. The negative deviations of susceptibility above about 100 K are due to occupancy of higher spin states. EPR spectra of **14** and **15** in THF at 4.5 K are essentially axial and are consistent with $S = 1/2$. (The spectrum of the related cluster $[Fe_4S_4(PBu^t{}_3)_3Cl]$ at 32 K is rhombic but corresponds to $S = 1/2$.[18]).

Lastly, the Mössbauer spectra of polycrystalline **14** and **16** consist of two quadrupole doublets in a 1:1 intensity ratio. The isomer shifts of the two clusters conform to those of the $[Fe_4S_4]^{1+}$ state. From the linear relationship between isomer shift and (mean) oxidation state for tetrahedral FeS_4 sites at 4.2 K,[1] $\delta = 0.59$ mm/s for a $[Fe_4S_4(SR)_4]^{3-}$ cluster. For FeS_4L sites, the isomer shifts decrease in the order $L = RS^- > R_3P$[29] such that values for $[Fe_4S_4(PR_3)_4]^{1+}$ are 0.46−0.51 mm/s, a lowering of 0.02−0.03 mm/s for each phosphine introduced. Subtraction of the effect of three phosphines from $\delta = 0.59$ mm/s gives 0.50 and 0.54 mm/s, in reasonable agreement with experimental values of 0.51 and 0.52 mm/s for thiolate-bound **14**. The same argument applies to **16**, confirming the mean oxidation state $Fe^{2.25+}$. The appearance of two quadrupole doublet accords with the prevailing theory of spin-coupling of $[Fe_4S_4]^{1+}$.[30,31] A Fe^{2+} Fe^{2+} pair ($S' = 4$) and a resonance delocalized $Fe^{2+}Fe^{3+}$ pair ($S' = 9/2$) are ferromagnetically coupled with the indicated spins, accounting for the two doublets. These pairs are antiferromagnetically coupled to produce the state $|9/2,4,1/2\rangle$ with $S = 1/2$ cluster spin.

With synthetic methods developed, solution solubility and stability conditions examined, and structural and ground state electronic properties revealed, we are in a favorable position to investigate site-specific reactivity, especially the potential of preparing higher nuclearity clusters. Such studies are in progress.

Acknowledgment. This research was supported by NIH Grant GM-28856. We thank Dr. R. Weber (Bruker BioSpin, Billerica, MA) for access to EPR equipment. This work made use of the MRSEC Shared Experimental Facilities at MIT, supported by the National Science Foundation under award number DMR-08-19762.

Supporting Information Available: X-ray crystallographic files in CIF form for all compounds in Tables 1 and 2. This material is available free of charge via the Internet at http://pubs.acs.org.

---

(23) Fee, J. A.; Castagnetto, J. M.; Case, D. A.; Noodleman, L.; Stout, C. D.; Torres, R. D. *J. Biol. Inorg. Chem.* **2003**, *8*, 519–526.

(24) Carney, M. J.; Papaefthymiou, G. C.; Spartalian, K.; Frankel, R. B.; Holm, R. H. *J. Am. Chem. Soc.* **1988**, *110*, 6084–6095.

(25) Carney, M. J.; Papaefthymiou, G. C.; Frankel, R. B.; Holm, R. H. *Inorg. Chem.* **1989**, *28*, 1497–1503.

(26) Yu., S.-B.; Papaefthymiou, G. C.; Holm, R. H. *Inorg. Chem.* **1991**, *30*, 3476–3485.

(27) Laskowski, E. J.; Frankel, R. B.; Gillum, W. O.; Papaefthymiou, G. C.; Renaud, J.; Ibers, J. A.; Holm, R. H. *J. Am. Chem. Soc.* **1978**, *100*, 5322–5337.

(28) Carney, M. J.; Holm, R. H.; Papaefthymiou, G. C.; Frankel, R. B. *J. Am. Chem. Soc.* **1986**, *108*, 3519–3521.

(29) Hauser, C.; Bill, E.; Holm, R. H. *Inorg. Chem.* **2002**, *41*, 1615–1624.

(30) Noodleman, L. *Inorg. Chem.* **1991**, *30*, 246–256.

(31) Mouesca, J.-M.; Noodleman, L.; Case, D. A.; Lamotte, B. *Inorg. Chem.* **1995**, *34*, 4347–4359.